

Diffusion on the circle and a stochastic correlation model

Sourav Majumdar

Department of Management Sciences, Indian Institute of Technology
Kanpur
souravm@iitk.ac.in
and
Arnab Kumar Laha
Operations and Decision Sciences, Indian Institute of Management
Ahmedabad
arnab@iima.ac.in

April 1, 2025

Abstract

We propose analytically tractable SDE models for correlation in financial markets. We study diffusions on the circle, namely the Brownian motion on the circle and the von Mises process, and consider these as models for correlation. The von Mises process was proposed in Kent 1975 as a probabilistic justification for the von Mises distribution which is widely used in Circular statistics. The transition density of the von Mises process has been unknown, we identify an approximate analytic transition density for the von Mises process. We discuss the estimation of these diffusion models and a stochastic correlation model in finance. We illustrate the application of the proposed model on real-data of equity-currency pairs.

Keywords: Directional Statistics, Statistical inference of continuous-time processes, von Mises process, Quantitative Finance

1 Introduction

A pertinent problem in quantitative finance is the joint modelling of multiple assets. Such issues arise in empirical analysis of financial data, portfolio optimization, and multi-asset derivatives pricing, among others. The usual modelling approach is to assume that the dependence between the assets is constant over time. However, empirical evidence suggests that correlation in stock markets is stochastic (Ball and Torous 2000; Driessen et al. 2009; Faria et al. 2022). This has led to significant interest towards the study of estimation of quadratic co-variance and its time varying nature, see Aït-Sahalia et al. 2010; Fan et al. 2016 and the references therein. One is also interested in parametric models for continuous-time correlation to perform no-arbitrage pricing of derivatives and forecasting. One of the first proposals to model continuous-time correlation was considered in Van Emmerich 2006, wherein a bounded functional of a Brownian motion was used to model correlation. Several extensions based on this approach have been considered Teng et al. 2015; Teng et al. 2016a; Teng et al. 2016b. Teng et al. 2018 consider a Jacobi process to model correlation. Another method to model covariance is via Wishart processes, which has also received a lot of attention in the literature Asai et al. 2006; Fonseca et al. 2007; Gourieroux and Sufana 2010; Philipov and Glickman 2006.

The transition probability density (TPD) of a diffusion is not always available in closed-form, which makes parametric inference of the diffusion difficult. This has led to significant interest towards the study of numerical and simulation based approaches to estimating the parameters of a diffusion, see Aït-Sahalia 2002; Beskos et al. 2006; Elerian et al. 2001; Kou et al. 2012. See Kalogeropoulos et al. 2011 for a simulation method for estimating correlated diffusions. For a recent survey see Craigmile et al. 2023.

Circular statistics studies data sampled from the unit circle, Jammalamadaka and Sen-

gupta 2001; Mardia and Jupp 2000. In this article, we study the estimation of some diffusions on the unit circle and explore a novel application to quantitative finance in stochastic correlation modelling. We consider two circular diffusions in this paper: the Circular Brownian Motion and the von Mises Process.

We are interested in estimating the parameters of a discretely observed circular diffusion through maximum likelihood estimation. The analytical form of the TPD of the von Mises process allows us to compute MLEs without relying on fully numerical or simulation approaches for the estimation of parameters of SDEs. Recently García-Portugués et al. 2019 also noted the lack of knowledge of TPD of the von Mises process in the literature. They proposed numerical approaches to estimate the von Mises process.

In this article, we consider a new approach to model correlation using circular diffusions. If X and Y are two random vectors in \mathbb{R}^n , then the Pearson correlation coefficient between X and Y is $\rho = \frac{\langle X, Y \rangle}{\|X\| \|Y\|} = \cos \theta$, where, $X = (x_1, x_2, \dots, x_n)$, $Y = (y_1, y_2, \dots, y_n)$, $\langle X, Y \rangle = \sum_{i=1}^n x_i y_i$ and $\|X\| = \sqrt{x_1^2 + x_2^2 + \dots + x_n^2}$. This leads to a natural choice to model ρ by modelling θ as a process on the circle. While ideas from circular statistics have been applied earlier to the statistical analysis of financial data (see SenGupta and Roy 2019; SenGupta and Roy 2023), the use of circular diffusion as a model for correlation has not been considered to the best of our knowledge.

The rest of the article is structured as follows. In Section 2 we discuss some background on diffusions on the circle. We derive an approximate transition density of the von Mises process and investigate its accuracy. In Section 3, we discuss the estimation of diffusions on the circle. We perform a simulation study and also perform real data analysis using them. In Section 4 we propose a stochastic correlation model, we discuss its estimation and a bootstrap procedure. In Section 5 we fit the proposed stochastic correlation model

to real financial data and discuss the analysis. In Section 6 we conclude the article.

2 Circular Diffusion

We first collect some known facts about Brownian motion on the circle. Let \mathbb{S}^1 denote the circle group, which is also a Lie group (see Stillwell 2008 for a background on Lie groups). Itô 1950 studied Brownian motion on Lie groups. Let θ denote the coordinate. For a Brownian motion on Lie group, it is shown that its transition density is uniquely characterized by its infinitesimal generator. $p(\theta_u; \theta_v)$ denotes the transition probability density function, i.e. the probability density of θ_u given θ_v , where θ_u is the position of the particle at time u . The infinitesimal generator (see Itô 1950, (1.2)) for a Brownian motion on the circle group is given by,

$$D = \frac{1}{2}\sigma^2 \frac{\partial^2}{\partial\theta^2} \quad (1)$$

and its forward equation (see Itô 1950, Theorem 2) is,

$$\frac{\partial}{\partial t}p(\theta_t; \theta_0) = Dp(\theta_t; \theta_0) \quad (2)$$

See Oksendal 2013, p. 117 for a definition of the infinitesimal generator. It is further shown that the paths of the Brownian motion on circle is continuous in the sense of Kolmogorov-Feller (Itô 1950) and its SDE representation is given by (Itô 1950, (2.6)),

$$d\theta_t = \sigma dB_t \quad (3)$$

where θ_t denotes the position of the Brownian motion on the circle at time t .

One can also characterize the Brownian motion on the circle alternatively, see Mardia and Jupp 2000, p. 51. Let $B_t, B_0 = 0$ denote the standard Brownian motion on \mathbb{R} . Then $\theta_t \in [0, 2\pi)$ is said to follow a circular Brownian motion as the process obtained by wrapping the Brownian motion on the circle, i.e., $\theta_t = (\sigma B_t \bmod 2\pi)$.

Equivalently it can also be characterized as following where θ_t is said to follow the circular Brownian motion if it satisfies the following SDE,

$$d\theta_t = \sigma dB_t \quad (4)$$

with periodic boundary conditions, $p(\theta_u; \theta_v) = p(\theta_u + 2k\pi; \theta_v)$, where $k \in \mathbb{Z}, u > v > 0$. The initial condition is $p_0(\theta) = \delta(\theta - 0)$, where δ denotes the Dirac-Delta function. The transition density is given in (10), by the Kolmogorov-Feller criterion the diffusion is continuous.

θ_t is said to follow the von Mises process (Kent 1975) if it satisfies the following SDE,

$$d\theta_t = -\lambda \sin(\theta_t - \mu) dt + \sigma dB_t \quad (5)$$

for $\lambda > 0, \sigma > 0$ and periodic boundary conditions.

The von Mises process was proposed as the circular analogue of the Ornstein-Uhlenbeck process on \mathbb{R} in Kent 1975. It is mean-reverting in the sense that the drift term $-\lambda \sin(\theta_t - \mu)$ pulls the particle θ_t towards the mean direction μ . It can be shown that the stationary distribution of the von Mises process is the von Mises distribution with density $f(\theta)$,

$$f(\theta) = \frac{1}{2\pi I_0(\kappa)} \exp(\kappa \cos(\theta - \mu)), 0 \leq \theta < 2\pi \quad (6)$$

where $\kappa = \frac{2\lambda}{\sigma^2}$ and $I_0(\cdot)$ is the zeroth-order modified Bessel function of the first kind. The von Mises distribution is widely used in circular statistics. To the best of our knowledge, no analytical solution of the TPD of the von Mises process has been reported in the literature. In this article, we present an approximate analytical solution for the TPD of the von Mises process.

Kent 1978 presented a construction through which one can obtain a time-reversible diffusion with a specified stationary distribution. We collect a special case of this construction in the following Lemma,

Lemma 2.1. *Let $f(\theta)$ be a strictly positive density on the circle, then the diffusion supported on the circle whose stationary density is $f(\theta)$ is given by,*

$$d\theta_t = \frac{1}{2} \frac{\partial}{\partial \theta_t} \log f(\theta_t) dt + \sigma dB_t \quad (7)$$

satisfying periodic boundary conditions.

Proof. See the appendix for a proof. \square

Applying Lemma 2.1, we construct the circular Brownian motion and the von Mises process.

For $f(x) = \frac{1}{2\pi}$, the density of the uniform distribution on the circle; applying Lemma 2.1 and the corresponding SDE given by,

$$d\theta_t = \sigma dB_t \quad (8)$$

alongwith the periodic boundary condition is referred to as the circular Brownian motion.

The forward equation for the circular Brownian motion is given by,

$$\frac{\partial}{\partial t} p(\theta_t; \theta_0) = \frac{\sigma^2}{2} \frac{\partial^2}{\partial \theta^2} p(\theta_t; \theta_0) \quad (9)$$

It can be checked by solving the forward equation of the circular Brownian motion (see (2)) that the transition density of θ_t , $0 < s < t$, is,

$$p(\theta_t; \theta_s) = \frac{1}{\sigma \sqrt{2\pi(t-s)}} \sum_{k=-\infty}^{\infty} \exp \left(\frac{-(\theta_t - \theta_s + 2k\pi)^2}{2\sigma^2(t-s)} \right). \quad (10)$$

which is the well-known wrapped normal distribution on the circle with parameters θ_s and $\sigma\sqrt{t-s}$, denoted by $\text{WN}(\theta_s, \sigma\sqrt{t-s})$. Thus, the stationary distribution of the circular

Brownian motion is the uniform distribution and the transition density is the wrapped normal distribution.

For $f(x) = \frac{1}{2\pi I_0(\kappa)} \exp(\kappa \cos(\theta - \mu))$, the density of the von Mises distribution with mean direction μ and concentration $\kappa = \frac{2\lambda}{\sigma^2}$, where λ is the mean-reversion parameter given in (11); applying Lemma 2.1 and the corresponding SDE is given by,

$$d\theta_t = -\lambda \sin(\theta_t - \mu) dt + \sigma dB_t \quad (11)$$

where $\theta, \mu \in [0, 2\pi)$, $\lambda, \sigma > 0$. This SDE is also referred to as the von Mises process.

The corresponding Kolmogorov-Forward equation is given by,

$$\frac{\partial}{\partial t} p(\theta_t; \theta_0) = \frac{\sigma^2}{2} \frac{\partial^2}{\partial \theta^2} p(\theta_t; \theta_0) + \lambda \sin(\theta_t - \mu) \frac{\partial}{\partial \theta} p(\theta_t; \theta_0) + \lambda \cos(\theta_t - \mu) p(\theta_t; \theta_0) \quad (12)$$

The stationary distribution of the von Mises process is the von Mises distribution as noted in its construction. However, the transition density of the von Mises process has not yet been reported in the literature.

2.1 Approximate transition density of von Mises process

We use the approximation framework presented in Martin et al. 2019 to obtain an approximate analytical solution for the forward equation of the von Mises process.

For deriving the approximate transition density of the von Mises process, we use the fact that the transition density of the Ornstein-Uhlenbeck process is known in closed form. A logarithmic transformation of the forward equation is considered, and the Ornstein-Uhlenbeck density then suggests an ansatz for more general forms of the drift term.

Therefore we state the following result,

Theorem 2.2.

$$p(\theta_t; \theta_0) \propto \sum_{k=-\infty}^{\infty} \exp \left(\frac{-\gamma \sqrt{q}(\theta_t + 2\pi k - \theta_0)^2}{2(1-q)} \right) \left(\frac{1}{2\pi I_0(\kappa)} \right)^{\frac{1-\sqrt{q}}{1+\sqrt{q}}} \exp \left(\frac{\kappa(\cos(\theta_t - \mu) - \sqrt{q} \cos(\theta_0 - \mu))}{1 + \sqrt{q}} \right) \quad (13)$$

where $\gamma = \kappa(I_1(\kappa)/I_0(\kappa))$ and $q = \exp(-\gamma\sigma^2 t)$. $p(\theta_t; \theta_0)$ is the approximate transition probability density of the von Mises process, in the sense that for $t \rightarrow 0$, the error term is $o(1)$ and for $t \rightarrow \infty$, $p(\theta; \theta_0, t) \rightarrow f_e$. Here f_e is the von Mises distribution.

Proof. See the appendix for a proof. \square

We note that as $t \rightarrow \infty$, $p(\theta_t; \theta_0) \rightarrow f_e$, which is the expected theoretical stationary distribution. The constant of proportionality ($C(\theta_0, \lambda, \sigma, \mu, t)$) can be obtained by numerically integrating $p(\theta; \theta_0, t)$ over θ , i.e.,

$$C(\theta_0, \lambda, \sigma, \mu, t) = \frac{1}{\int p(\theta_t; \theta_0) d\theta} \quad (14)$$

2.2 Numerical experiment

In (13) we obtain an approximate analytical solution of the von Mises process. To validate the accuracy of the approximate analytical solution we compare it with a numerical solution of the transition probability density.

One possible approach is to solve the forward equation (12) numerically. Towards this a standard approach is the Crank-Nicholson scheme which was also considered in Section 3.4.1, García-Portugués et al. 2019. In this approach a uniform discretization of the space, i.e., $(-\pi, \pi]$ is considered into k points and similarly time $(0, T]$ is discretized uniformly into m points. The PDE is also further discretized and the resulting numerical estimate of the density is obtained at these k points for each m time points. The reader may refer

to Section 3.4.1, García-Portugués et al. 2019 for an exposition of the Crank-Nicholson scheme.

Let p and q denote two probability density functions, then the Hellinger distance (see Le Cam and Yang 2000) is defined as,

$$h(p, q) = \frac{1}{\sqrt{2}} \sqrt{\int_{\mathbb{R}} (\sqrt{dp} - \sqrt{dq})^2} \quad (15)$$

Hellinger distance is used to quantify the similarity between two probability densities. It is known that $0 \leq h(p, q) \leq 1$, where if $h(p, q)$ is close to 0, then p and q are interpreted to be similar.

Let p denote the density of the approximate analytical solution and let q denote the density of the numerical solution. Since the numerical solution q via the Crank-Nicholson scheme is discrete, we consider the discrete version of the Hellinger distance by discretizing p at the same k points. This is given by,

$$h(p, q) = \frac{1}{\sqrt{2}} \sqrt{\sum_{i=1}^k (\sqrt{p_i} - \sqrt{q_i})^2} \quad (16)$$

We use the function `dTpPdPde1D` in the R package `sdetorus` (García-Portugués 2023) to utilize the implementation of Crank-Nicholson scheme to numerically solve the forward equation of the von Mises process. We compare analytical approximate solution $p(\theta; \theta_0, t)$ (13) with the numerical solution via the Hellinger distance between them. We set $k = 3000, m = 20000$ for the Crank-Nicholson scheme. We set $\theta_0 = 0$ and we compare the densities after time t has elapsed, where $t \in \{0.0001, 0.001, 0.01, 0.1\}$ for varying $\mu \in \{-\frac{\pi}{2}, -\frac{\pi}{3}, -\frac{\pi}{4}, \frac{\pi}{4}, \frac{\pi}{3}, \frac{\pi}{2}\}$. For each t and μ we also evaluate the Hellinger distance for different values of κ , i.e., $\kappa = 0.5$ ($\lambda = 1, \sigma = 2$), $\kappa = 1$ ($\lambda = 2, \sigma = 1$), $\kappa = 2$ ($\lambda = 1, \sigma = 2$) and $\kappa = 4$ ($\lambda = 2, \sigma = 2$). We report the results in Figure 1. We find that for all cases considered the Hellinger distance is very low ($\lesssim 0.01$), which indicates the accuracy of the

approximate analytical solution.

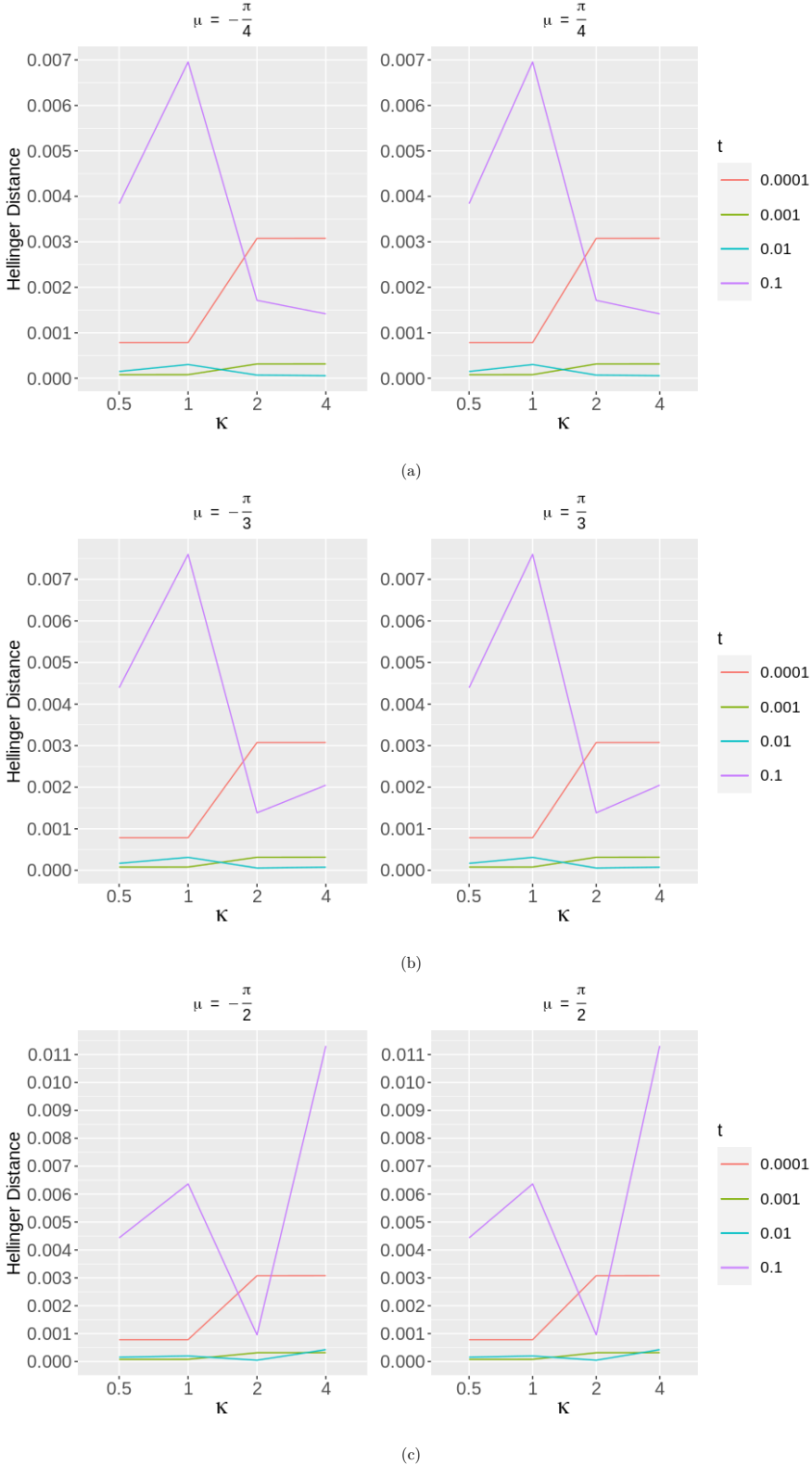


Figure 1: Hellinger distance between the analytical ($p(\theta; \theta_0, t)$) and numerical approximation of the forward equation of the von Mises process. The parameters are $\theta_0 = 0$ and $\kappa = 0.5$ ($\lambda = 1, \sigma = 2$), $\kappa = 1$ ($\lambda = 2, \sigma = 1$), $\kappa = 2$ ($\lambda = 1, \sigma = 2$) and $\kappa = 4$ ($\lambda = 2, \sigma = 2$). We compare the Hellinger distance at $\mu = -\frac{\pi}{2}, -\frac{\pi}{3}, -\frac{\pi}{4}, \frac{\pi}{4}, \frac{\pi}{3}, \frac{\pi}{2}$. For a given μ we plot the Hellinger distance between the numerical and the analytical density for different values of t , where t is the time elapsed. For the Crank-Nicholson scheme for the numerical solution we set $k = 3000, m = 20000$. 11

3 Estimation of Circular Diffusions

In this section we consider the estimation of a discretely observed Circular diffusion. Let θ_t be a circular diffusion and we observe θ_t at times $0 = t_1 < t_2 < \dots < t_n = T$. We consider the case where θ_t is the circular Brownian motion and the von Mises process.

The quadratic variation of θ_t , where θ_t could be either the circular Brownian motion or the von Mises process, is given by,

$$[\theta]_t = \int_0^T \sigma^2 dt \quad (17)$$

Hence, $\sigma^2 = \frac{[\theta]_T}{T}$. The sample quadratic variation estimator is given by,

$$[\theta]_t^* = \sum_{i=1}^{n-1} (\theta_i^*)^2 \quad (18)$$

where $\theta_i^* = (\theta_{t_{i+1}} - \theta_{t_i}) \bmod \pi$. It is known that $[\theta]_t^* \xrightarrow{ucp} [\theta]_t$ as $\sup_i |t_{i+1} - t_i| \rightarrow 0$, see Protter 2005, Theorem 22, p. 66. Therefore the diffusion coefficient estimator is,

$$\hat{\sigma}^2 = \frac{[\theta]_T^*}{T} \quad (19)$$

If $\sup_i |t_{i+1} - t_i|$ is sufficiently small, i.e. we sample from the diffusion very frequently, then the estimator is expected to perform well.

We note that the consistency and asymptotic normality of the maximum likelihood estimation (MLE) of a discretely observed Itô process has been established, see Prakasa Rao 1983; Yoshida 1992. To estimate the parameters in the drift term of the von Mises process, i.e. λ, μ , we propose to perform numerical estimates of the parameters. We are unable to obtain analytical solutions for λ, μ since we know (13) only upto proportionality. A promising approach to estimating parameters of non-normalized models is the score matching estimator, see Hyvärinen and Dayan 2005; Mardia, Kent, and Laha 2016. The

score-matching formulation for this model was tried but proved to be not analytically tractable for us.

The log-likelihood of the von-Mises process is given by,

$$l(\lambda, \mu; \theta) = \sum_{i=1}^{n-1} C_i p(\theta_{i+1}; \theta_i, t) \quad (20)$$

where C_i is a shorthand for $C(\theta_i, \lambda, \sigma, \mu, t_i)$ and we use $\hat{\sigma}$ as a plugin estimator for the diffusion coefficient. Then $\arg \max_{\lambda, \mu} l$ to obtain the estimates for λ, μ .

3.1 Simulation study

We evaluate the performance of the estimating procedure by simulating from both the circular Brownian motion and the von Mises process. We simulate from the circular Brownian motion and the von Mises process utilizing the Euler-Maruyama discretization of their SDEs and wrapping it. See Kloeden and Platen 1992 for a background on Euler-Maruyama discretization. We vary both the sample size n (i.e., the number of observations) and the time step Δt between observations. For each setting, we generate 100 simulated paths and estimate the parameters on each path. In the tables below, we report the empirical bias and the standard deviation of that difference across the 100 replications.

For the circular Brownian motion we vary σ in $\{1, 2\}$, n in $\{1000, 5000, 10000\}$ and Δt in $\{0.005, 0.05, 0.5\}$. We report the results in Table 1. We observe that the Bias of the $\hat{\sigma}$ is close to 0 in general. The variance of $\sigma - \hat{\sigma}$ decreases as n increases and Δt decreases. For the circular Brownian motion simulations, the quadratic variation estimator for σ performs very well, displaying minimal bias and decreasing variance with increasing n .

σ	n	Δt	$\mathbb{E}[\sigma - \hat{\sigma}]$	$\sqrt{\text{Var}[\sigma - \hat{\sigma}]}$
1	1000	0.5	0.001	0.023
1	1000	0.05	0.001	0.023
1	1000	0.005	0.000	0.021
1	5000	0.5	-0.001	0.010
1	5000	0.05	0.000	0.008
1	5000	0.005	0.003	0.010
1	10000	0.5	0.001	0.007
1	10000	0.05	0.001	0.006
1	10000	0.005	0.000	0.007
2	1000	0.5	0.078	0.042
2	1000	0.05	0.002	0.047
2	1000	0.005	-0.009	0.047
2	5000	0.5	0.083	0.014
2	5000	0.05	0.001	0.022
2	5000	0.005	-0.003	0.019
2	10000	0.5	0.083	0.010
2	10000	0.05	0.002	0.013
2	10000	0.005	-0.001	0.015

Table 1: Simulation results for the circular Brownian motion. Columns report the empirical mean (bias) and standard deviation (SD) of $\sigma - \hat{\sigma}$ across 100 simulated paths for each combination of σ , n , and Δt .

We next consider von Mises process simulations, where the true parameters are μ, λ , and σ . We again vary n in $\{1000, 5000, 10000\}$ and Δt in $\{0.005, 0.05, 0.5\}$. We vary the parameter configurations as follows where, $\mu \in \left\{-\frac{\pi}{2}, \frac{\pi}{2}\right\}$, $\lambda \in \{1, 2\}$, $\sigma \in \{1, 2\}$. We report the results for von Mises process in Table 2 for $\Delta t = 0.005$, in Table 3 for $\Delta t = 0.05$ and Table 4 for $\Delta t = 0.5$. We measure the bias and the standard deviation of the difference

between the true parameter and estimated parameter for λ and σ . Since, μ is a circular variable we measure its bias and concentration by,

$$\text{Bias} = \text{atan2}(S, C)$$

$$\text{Concentration} = \sqrt{S^2 + C^2}$$

where $S = \sum_{k=1}^{100} \sin(\mu - \hat{\mu}_k)$ and $C = \sum_{k=1}^{100} \cos(\mu - \hat{\mu}_k)$.

A good estimator of μ should possess a low value of Bias, i.e. close to 0 and a high value of Concentration , i.e. close to 1.

We observe that, bias in $\hat{\lambda}$ and $\hat{\mu}$ is larger for smaller n , improving as n increases. $\hat{\sigma}$ for the von Mises process also shows minimal bias. As Δt grows larger and n is small, the drift parameter $\hat{\lambda}$ shows moderate estimation error. This is because there are fewer data points to capture the mean-reversion behavior well. The bias of $\hat{\mu}$ shrinks with increasing n , and the concentration metric nears 1, indicating accurate estimates of μ .

μ	λ	σ	n	$\mathbb{E}[\lambda - \hat{\lambda}]$	$\sqrt{\text{Var}[\lambda - \hat{\lambda}]}$	$\mathbb{E}[\sigma - \hat{\sigma}]$	$\sqrt{\text{Var}[\sigma - \hat{\sigma}]}$	Bias of $\hat{\mu}$	Concentration of $\mu - \hat{\mu}$
$-\pi/2$	1	1	1000	-1.385	1.501	0.002	0.023	-0.179	0.787
$-\pi/2$	1	2	1000	-1.094	1.232	0.002	0.042	-0.291	0.471
$-\pi/2$	2	1	1000	-1.346	1.562	-0.001	0.023	-0.087	0.947
$-\pi/2$	2	2	1000	-1.053	1.463	0.000	0.042	0.021	0.784
$\pi/2$	1	1	1000	-1.400	1.452	0.000	0.022	0.243	0.757
$\pi/2$	1	2	1000	-1.051	1.367	0.001	0.048	0.072	0.514
$\pi/2$	2	1	1000	-1.384	1.433	0.000	0.023	0.074	0.938
$\pi/2$	2	2	1000	-1.050	1.511	-0.002	0.048	0.073	0.803
$-\pi/2$	1	1	5000	-0.692	0.533	-0.001	0.009	-0.064	0.954
$-\pi/2$	1	2	5000	-0.360	0.545	-0.004	0.021	-0.212	0.855
$-\pi/2$	2	1	5000	-1.014	0.714	-0.002	0.009	-0.022	0.991
$-\pi/2$	2	2	5000	-0.316	0.678	-0.001	0.020	-0.072	0.969
$\pi/2$	1	1	5000	-0.612	0.575	-0.002	0.010	0.028	0.955
$\pi/2$	1	2	5000	-0.381	0.557	-0.004	0.019	0.185	0.822
$\pi/2$	2	1	5000	-1.018	0.776	-0.003	0.010	0.012	0.990
$\pi/2$	2	2	5000	-0.446	0.644	-0.004	0.021	0.067	0.966
$-\pi/2$	1	1	10000	-0.578	0.355	-0.001	0.008	-0.003	0.983
$-\pi/2$	1	2	10000	-0.246	0.440	0.001	0.015	-0.273	0.939
$-\pi/2$	2	1	10000	-0.999	0.510	-0.001	0.007	-0.002	0.996
$-\pi/2$	2	2	10000	-0.298	0.519	-0.003	0.014	-0.076	0.984
$\pi/2$	1	1	10000	-0.609	0.434	-0.001	0.008	0.022	0.981
$\pi/2$	1	2	10000	-0.161	0.402	-0.003	0.016	0.216	0.910
$\pi/2$	2	1	10000	-0.946	0.442	-0.002	0.007	0.016	0.996
$\pi/2$	2	2	10000	-0.341	0.487	-0.003	0.013	0.088	0.986

Table 2: Simulation results for the von Mises process for $\Delta t = 0.005$. Columns report the bias and the standard deviation of $\lambda - \hat{\lambda}$ and $\sigma - \hat{\sigma}$. We also report the bias and concentration for $\hat{\mu}$, see section 3.1 for their definitions.

μ	λ	σ	n	$\mathbb{E}[\lambda - \hat{\lambda}]$	$\sqrt{\text{Var}[\lambda - \hat{\lambda}]}$	$\mathbb{E}[\sigma - \hat{\sigma}]$	$\sqrt{\text{Var}[\sigma - \hat{\sigma}]}$	Bias of $\hat{\mu}$	Concentration of $\mu - \hat{\mu}$
$-\pi/2$	1	1	1000	-0.131	0.254	-0.002	0.022	-0.059	0.989
$-\pi/2$	1	2	1000	-0.226	0.420	-0.004	0.044	-0.294	0.926
$-\pi/2$	2	1	1000	-0.156	0.311	-0.021	0.023	-0.010	0.997
$-\pi/2$	2	2	1000	-0.308	0.497	-0.022	0.042	-0.113	0.986
$\pi/2$	1	1	1000	-0.154	0.247	-0.007	0.022	0.032	0.989
$\pi/2$	1	2	1000	-0.341	0.460	-0.008	0.047	0.198	0.927
$\pi/2$	2	1	1000	-0.145	0.325	-0.020	0.022	0.006	0.997
$\pi/2$	2	2	1000	-0.204	0.487	-0.021	0.046	0.095	0.984
$-\pi/2$	1	1	5000	-0.094	0.108	-0.009	0.009	-0.020	0.997
$-\pi/2$	1	2	5000	-0.159	0.223	-0.007	0.021	-0.253	0.988
$-\pi/2$	2	1	5000	-0.079	0.119	-0.021	0.009	0.000	0.999
$-\pi/2$	2	2	5000	-0.276	0.235	-0.023	0.021	-0.105	0.997
$\pi/2$	1	1	5000	-0.098	0.104	-0.008	0.011	0.019	0.997
$\pi/2$	1	2	5000	-0.174	0.188	-0.006	0.019	0.252	0.988
$\pi/2$	2	1	5000	-0.084	0.136	-0.023	0.009	0.006	0.999
$\pi/2$	2	2	5000	-0.230	0.202	-0.022	0.018	0.110	0.997
$-\pi/2$	1	1	10000	-0.090	0.074	-0.010	0.007	-0.022	0.999
$-\pi/2$	1	2	10000	-0.153	0.148	-0.007	0.013	-0.248	0.995
$-\pi/2$	2	1	10000	-0.058	0.080	-0.021	0.007	-0.001	1.000
$-\pi/2$	2	2	10000	-0.228	0.139	-0.023	0.013	-0.107	0.999
$\pi/2$	1	1	10000	-0.087	0.076	-0.009	0.008	0.028	0.999
$\pi/2$	1	2	10000	-0.140	0.161	-0.005	0.013	0.270	0.995
$\pi/2$	2	1	10000	-0.073	0.089	-0.023	0.007	0.004	1.000
$\pi/2$	2	2	10000	-0.239	0.144	-0.023	0.015	0.105	0.999

Table 3: Simulation results for the von Mises process for $\Delta t = 0.05$. Columns report the bias and the standard deviation of $\lambda - \hat{\lambda}$ and $\sigma - \hat{\sigma}$. We also report the bias and concentration for $\hat{\mu}$, see section 3.1 for their definitions.

μ	λ	σ	n	$\mathbb{E}[\lambda - \hat{\lambda}]$	$\sqrt{\text{Var}[\lambda - \hat{\lambda}]}$	$\mathbb{E}[\sigma - \hat{\sigma}]$	$\sqrt{\text{Var}[\sigma - \hat{\sigma}]}$	Bias of $\hat{\mu}$	Concentration of $\mu - \hat{\mu}$
$-\pi/2$	1	1	1000	-0.079	0.099	-0.093	0.028	-0.056	0.999
$-\pi/2$	1	2	1000	0.106	0.168	0.041	0.034	-0.364	0.984
$-\pi/2$	2	1	1000	-0.273	0.108	-0.286	0.032	-0.019	1.000
$-\pi/2$	2	2	1000	0.441	0.191	-0.082	0.042	-0.175	0.995
$\pi/2$	1	1	1000	-0.080	0.078	-0.095	0.026	0.040	0.999
$\pi/2$	1	2	1000	0.113	0.164	0.035	0.039	0.316	0.976
$\pi/2$	2	1	1000	-0.259	0.100	-0.284	0.030	0.023	1.000
$\pi/2$	2	2	1000	0.414	0.198	-0.077	0.033	0.190	0.994
$-\pi/2$	1	1	5000	-0.083	0.037	-0.096	0.011	-0.054	1.000
$-\pi/2$	1	2	5000	0.161	0.078	0.040	0.014	-0.340	0.997
$-\pi/2$	2	1	5000	-0.269	0.044	-0.287	0.014	-0.016	1.000
$-\pi/2$	2	2	5000	0.433	0.075	-0.079	0.017	-0.193	0.999
$\pi/2$	1	1	5000	-0.071	0.036	-0.096	0.012	0.056	1.000
$\pi/2$	1	2	5000	0.144	0.081	0.038	0.017	0.340	0.997
$\pi/2$	2	1	5000	-0.270	0.056	-0.287	0.013	0.018	1.000
$\pi/2$	2	2	5000	0.426	0.087	-0.079	0.017	0.189	0.999
$-\pi/2$	1	1	10000	-0.074	0.026	-0.095	0.008	-0.048	1.000
$-\pi/2$	1	2	10000	0.152	0.055	0.038	0.012	-0.345	0.998
$-\pi/2$	2	1	10000	-0.265	0.037	-0.286	0.010	-0.018	1.000
$-\pi/2$	2	2	10000	0.435	0.054	-0.079	0.012	-0.192	1.000
$\pi/2$	1	1	10000	-0.076	0.025	-0.096	0.008	0.047	1.000
$\pi/2$	1	2	10000	0.152	0.058	0.038	0.010	0.349	0.998
$\pi/2$	2	1	10000	-0.261	0.029	-0.287	0.009	0.019	1.000
$\pi/2$	2	2	10000	0.431	0.063	-0.080	0.013	0.189	0.999

Table 4: Simulation results for the von Mises process for $\Delta t = 0.5$. Columns report the bias and the standard deviation of $\lambda - \hat{\lambda}$ and $\sigma - \hat{\sigma}$. We also report the bias and concentration for $\hat{\mu}$, see section 3.1 for their definitions.

Overall the simulation study confirms that the quadratic-variation-based estimator for σ is accurate for both the circular Brownian motion and the von Mises process. The approximate MLE strategy for the von Mises process (using the derived transition density approximation) performs well, with parameter estimates converging as n increases and as Δt becomes smaller.

3.2 Real data analysis

We now illustrate an application of the estimation of the above models to wind direction data. The following data is obtained from a wind-power farm named “Sotavento Galicia”, located in Spain. We also refer to it as Sotavento Wind Farm in this paper. Sotavento Wind Farm makes available the data for wind direction at their farm, Sotavento Galicia 2024. The data from the Sotavento wind farm has been previously analyzed in the literature, see Khazaei et al. 2022. The analysis of wind data is relevant for evaluating the economic and technical viability of wind power projects.

In our analysis we obtain wind direction data from Sotavento Wind farm at a 10 minute frequency from 1 November 2024 to 30 November 2024. We plot the time series of this wind direction data in Figure 2.

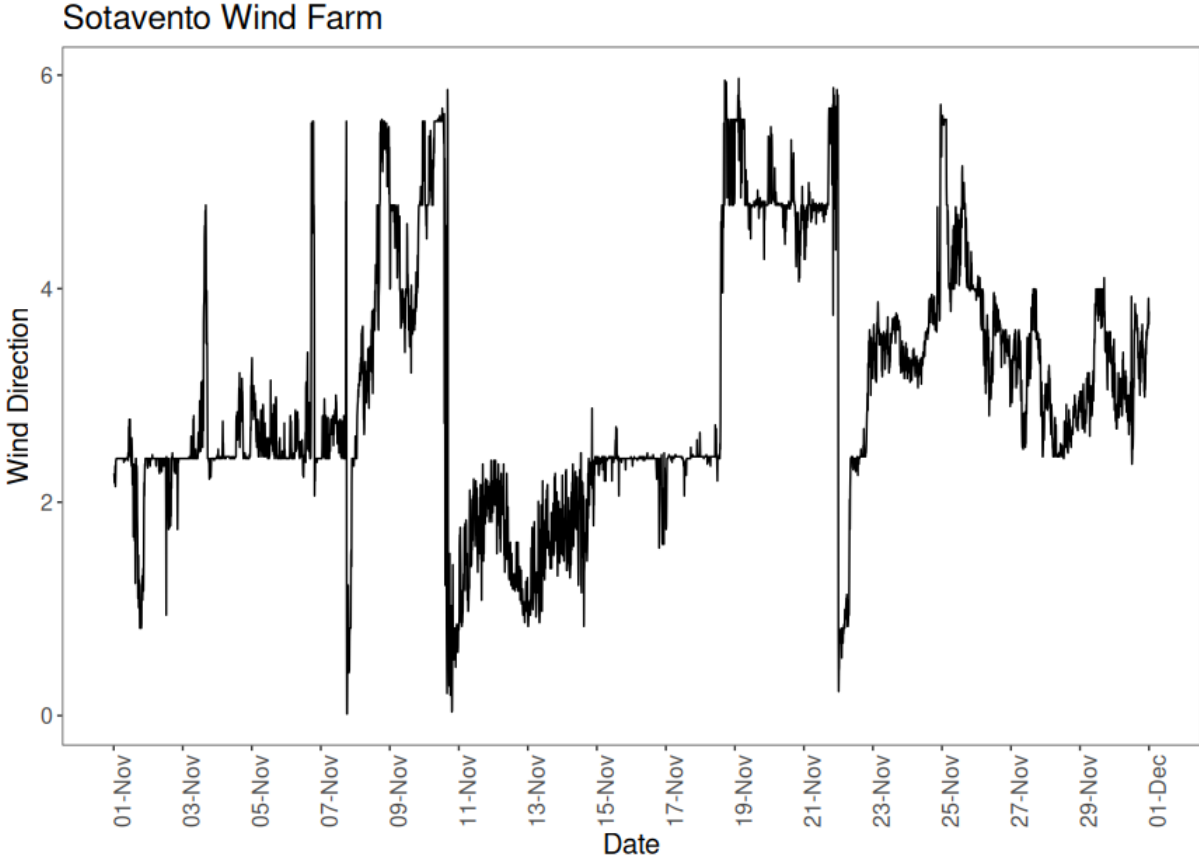


Figure 2: Wind direction data in radians from 1 November 2024 to 30 November 2024 at a 10 minute frequency.

We fit both the circular Brownian motion and the von Mises process to this data. Let θ_t denote the wind-direction at time t . The circular Brownian motion model is given by,

$$d\theta_t = \sigma_{\text{bm}} dW_t$$

and the von Mises process model is given by,

$$d\theta_t = -\lambda_{\text{vm}} \sin(\theta_t - \mu_{\text{vm}}) dt + \sigma_{\text{vm}} dW_t$$

As per the notation above $t_{i+1} - t_i = 10$ minutes, $\forall i$. Therefore $\Delta t = t_{i+1} - t_i = \frac{10}{1440}$ days.

We report that $\hat{\sigma}_{\text{bm}} = 2.96$. For the von Mises process, the estimates are $\hat{\sigma}_{\text{vm}} = 2.96$, $\hat{\lambda}_{\text{vm}} = 4.60$ and $\hat{\mu}_{\text{vm}} = 2.61$. The estimated $\hat{\sigma}_{\text{bm}}$ and $\hat{\sigma}_{\text{vm}}$ are identical because both were obtained via the quadratic variation estimator. We also obtain the 95% confidence region for the parameters using parametric bootstrap. We describe the parametric bootstrap procedure for the stochastic correlation model in Algorithm 1.

The 95% confidence region for $\hat{\sigma}_{\text{bm}}$ is $(2.90, 3.02)$ and for $\hat{\sigma}_{\text{vm}}$ is $(2.89, 3.01)$. We note that under both models the estimated volatility coefficient and their intervals are nearly identical. The 95% confidence region for $\hat{\mu}_{\text{vm}}$ is $(2.11, 3.11)$. The 95% confidence interval for $\hat{\lambda}_{\text{vm}}$ is $(3.25, 6.74)$. This indicates a mean-reverting behavior of the wind-direction at the Sotavento farm.

4 A stochastic correlation model

In this section we propose to model stochastic correlation in financial markets using the circular diffusions described above. We also consider the estimation of such a model.

Let $S_t^{(1)}$ and $S_t^{(2)}$ describe the price of two assets at time t . We assume that the price dynamics of $S_t^{(1)}$ and $S_t^{(2)}$ follow a correlated geometric Brownian motion. Geometric Brownian motion is a benchmark stock price model due to its analytical tractability, other suitable price processes can also be considered. We describe the dynamics below,

$$\begin{aligned} dS_t^{(1)} &= \mu^{(1)} S_t^{(1)} dt + \sigma^{(1)} S_t^{(1)} dB_t^{(1)} \\ dS_t^{(2)} &= \mu^{(2)} S_t^{(2)} dt + \sigma^{(2)} S_t^{(2)} \left(\rho_t dB_t^{(1)} + \sqrt{1 - \rho_t^2} dB_t^{(2)} \right) \end{aligned} \quad (21)$$

where $\rho_t = \cos \theta_t$, with two possible choices for modelling θ_t being the circular Brownian motion ($d\theta_t = \sigma dB_t^{(3)}$) and the von Mises process ($d\theta_t = -\lambda \sin(\theta_t - \mu) dt + \sigma dB_t^{(3)}$).

Here $B_t^{(1)}, B_t^{(2)}, B_t^{(3)}$ are mutually independent standard Brownian motion process. In this specification, note that the correlation process is independent from the price process. This assumption can be relaxed at the cost of some loss in tractability during estimation.

Theorem 4.1. *The strong solution to SDEs (21) model exists.*

Proof. See the appendix for a proof. \square

4.1 Estimation

In this model note that ρ_t is a latent variable. Filtering based approaches are usually used for estimation in models with latent variables, see Lautier et al. 2003. However we can write down the likelihood in closed form and use it to estimate the model parameters. Typically one is also interested in the measurement of the underlying latent variable. We propose a method with which one can estimate the parameters and recover the most likely realization of the correlation process.

Suppose we observe the asset prices in $t \in [0, T]$ at a frequency of Δt . The vector of observations is given by $\mathbf{S}^{(1)} = \{S_0^{(1)}, S_{\Delta t}^{(1)}, \dots, S_{T-\Delta t}^{(1)}, S_T^{(1)}\}$. $\mathbf{S}^{(2)} = \{S_0^{(2)}, S_{\Delta t}^{(2)}, \dots, S_{T-\Delta t}^{(2)}, S_T^{(2)}\}$. There is also a realization of the correlation dynamic which remains unobserved and we denote it by, $\boldsymbol{\rho} = \{\rho_0, \rho_{\Delta t}, \dots, \rho_{T-\Delta t}, \rho_T\}$.

It can be shown that the log-likelihood of the asset price conditional on the correlation is given by,

$$\tilde{L}(\mu^{(1)}, \sigma^{(1)}, \mu^{(2)}, \sigma^{(2)}; \mathbf{S}^{(1)}, \mathbf{S}^{(2)}, \boldsymbol{\rho}) = \sum_{i=0}^{T/\Delta t} -\frac{1}{2} \left((\log \mathbf{S}_i - \mathbf{M})^T \boldsymbol{\Sigma}_i^{-1} (\log \mathbf{S}_i - \mathbf{M}) + \log(|\boldsymbol{\Sigma}_i|) \right) \quad (22)$$

where $\mathbf{S}_i = \{S_{i\Delta t}^{(1)}, S_{i\Delta t}^{(2)}\}$ and $\mathbf{M} = \{\mu^{(1)} - \frac{(\sigma^{(1)})^2}{2}, \mu^{(2)} - \frac{(\sigma^{(2)})^2}{2}\}$. The covariance matrix

Σ_i is given by,

$$\Sigma_i = \begin{bmatrix} (\sigma^{(1)})^2 \Delta t & \sigma^{(1)} \sigma^{(2)} \rho_{(i\Delta t)} \Delta t \\ \sigma^{(1)} \sigma^{(2)} \rho_{(i\Delta t)} \Delta t & (\sigma^{(2)})^2 \Delta t \end{bmatrix}$$

Since the correlation process is independent of the asset price process, joint log likelihood is given by,

$$\begin{aligned} L(\mu^{(1)}, \sigma^{(1)}, \mu^{(2)}, \sigma^{(2)}, \boldsymbol{\rho}, \lambda, \sigma; \mathbf{S}^{(1)}, \mathbf{S}^{(2)}) \\ = \sum_{i=0}^{T/\Delta t} -\frac{1}{2} \left((\log \mathbf{S}_i - \mathbf{M})^T \Sigma_i^{-1} (\log \mathbf{S}_i - \mathbf{M}) + \log(|\Sigma_i|) \right) \\ + \log p(\cos^{-1}(\rho_{(i+1)\Delta t}); \cos^{-1}(\rho_{i\Delta t}), \Delta t) \\ - \log \sqrt{1 - \rho_{(i+1)\Delta t}^2} \end{aligned}$$

We maximize L , to obtain the estimates. Here p denotes the transition density of the chosen process, if the correlation process is the circular Brownian motion then p is given by (10) or if the correlation process is the von Mises process then p is given by (13).

For the von Mises process, we found that penalizing large values of κ led to better results. We do this for computational reasons. We need to evaluate $I_1(\kappa)$ and $I_0(\kappa)$, the modified Bessel functions, a very large value of κ would make it numerically infeasible to evaluate these functions. We choose a penalization term for κ in proportion to the size of the data, where for more observations we would increase the penalization value. We also wanted to minimize large variations in inter-period correlation estimates, which otherwise would be inconsistent with economic intuition, therefore we also considered adding a penalizing term for both the circular Brownian motion and von Mises process. Therefore we finally consider a penalized version of the likelihood that we use to estimate the parameters,

$$L^*(\mu_1, \sigma_1, \mu_2, \sigma_2, \boldsymbol{\rho}, \lambda, \sigma; \mathbf{S}^{(1)}, \mathbf{S}^{(2)}) = L + \lambda_1 \left(\frac{T}{\Delta t} \right) \sum_{i=0}^{T/\Delta t} (\rho_{(i+1)\Delta t} - \rho_{i\Delta t})^2 + \lambda_2 \kappa \quad (23)$$

where $\lambda_2 = 0$, if the circular Brownian motion is being considered. We perform the maximization of L^* using the Constrained Optimization by Linear Approximation (COBYLA) algorithm, Powell 1998, which is an iterative optimization procedure. At each iteration step we use the quadratic variation estimator (19) to estimate σ from the present estimate of ρ , since the correlation process is independent of the price process. We utilize the implementation of the algorithm in the R package **NOpt** (Johnson 2007).

4.2 Bootstrap

Since we work with penalized likelihood to estimate the model, the asymptotic normality of MLE is unavailable to quantify the uncertainty of the estimates. We perform parametric bootstrap (see p. 306, Efron and Tibshirani 1994) to get confidence interval for the estimates of ρ .

We recall a result from Ducharme et al. 1985; Fisher and Hall 1989 regarding the choice of pivot for bootstrap for circular random variables. Let $\theta_1, \theta_2, \dots, \theta_n$ denote the random sample of a circular random variable. Let $\hat{\alpha}$ be a circular estimate of a parameter from the sample. Define, $U(\hat{\alpha}, \alpha) = 1 - \cos(\hat{\alpha} - \alpha)$. Upon Bootstrap resampling, we obtain values $U(\hat{\alpha}, \alpha_1), U(\hat{\alpha}, \alpha_2), \dots, U(\hat{\alpha}, \alpha_n)$. Then the $100 \times q$ -th percentile value of U is chosen corresponding to which we obtain α_q . Then $\theta_q = \hat{\alpha} - \alpha_q$, and therefore the confidence region for $\hat{\alpha}$ is $\hat{\alpha} \pm \alpha_q$.

Following this we propose $U^*(\hat{\rho}, \rho) = 1 - \cos(\cos^{-1}(\hat{\rho}) - \cos^{-1}(\rho))$ as the pivot for bootstrapping estimated correlation. Let U_q^* denote the $100 \times q$ -th percentile value, then the q -th confidence region for $\hat{\rho}$ is $\hat{\rho} \pm U_q^*$.

The bootstrap procedure is described in Algorithm 1.

Algorithm 1 Bootstrap confidence region for ρ

- **Input:** $\hat{\mu}^{(1)}, \hat{\sigma}^{(1)}, \hat{\mu}^{(2)}, \hat{\sigma}^{(2)}, \hat{\rho} = \{\hat{\rho}_0, \hat{\rho}_{\Delta t}, \hat{\rho}_{2\Delta t}, \dots, \hat{\rho}_T\}$. Parameters of the circular diffusion process: circular Brownian motion ($\hat{\sigma}$) or von Mises process ($\hat{\lambda}, \hat{\mu}, \hat{\sigma}$).

- **Parameters:** N : the number of bootstrap samples.

- **Output:** Bootstrap confidence region for ρ .

- 1: Generate N random samples from $S_t^{(1)}$ and $S_t^{(2)}$ at times $t = \{0, \Delta t, 2\Delta t, \dots, T\}$ using the estimated parameters as input. Then for each $i \in \{1, 2, \dots, N\}$, $\mathbf{S}^{(1)i} = \{S_0^{(1)i}, S_{\Delta t}^{(1)i}, \dots, S_T^{(1)i}\}$ and $\mathbf{S}^{(2)i} = \{S_0^{(2)i}, S_{\Delta t}^{(2)i}, \dots, S_T^{(2)i}\}$
- 2: For each i , we estimate the model for $\mathbf{S}^{(1)i}$ and $\mathbf{S}^{(2)i}$, corresponding to which we obtain an estimate $\hat{\rho}^i = \{\hat{\rho}_0^i, \hat{\rho}_{\Delta t}^i, \dots, \hat{\rho}_T^i\}$.
- 3: Then for each $t^* \in \{0, \Delta t, \dots, T\}$, compute $U(\hat{\rho}_{t^*}, \hat{\rho}_{t^*}^1), U(\hat{\rho}_{t^*}, \hat{\rho}_{t^*}^2), \dots, U(\hat{\rho}_{t^*}, \hat{\rho}_{t^*}^N)$. Let $U_q^{t^*}$ denote the $100 \times q$ -th percentile value of these U 's.
- 4: Then the q -th confidence region for $\hat{\rho}_{t^*}$ is $\hat{\rho}_{t^*} \pm U_q^{t^*}$.

Proposition 4.1. *We note that the solution of the stochastic correlation model is given by,*

$$S_t^{(1)} = S_0^{(1)} \exp \left(\left(\mu^{(1)} - \frac{(\sigma^{(1)})^2}{2} \right) t + \sigma^{(1)} B_t^{(1)} \right)$$

$$S_t^{(2)} = S_0^{(2)} \exp \left(\left(\mu^{(2)} - \frac{(\sigma^{(2)})^2}{2} \right) t + \sigma^{(2)} (\rho_t B_t^{(1)} + \sqrt{1 - \rho_t^2} B_t^{(2)}) \right)$$

We can plugin the estimates $\hat{\mu}^{(1)}, \hat{\sigma}^{(1)}, \hat{\mu}^{(2)}, \hat{\sigma}^{(2)}, \hat{\rho}$ to simulate from the model as is needed for Step 1 of the Bootstrap algorithm.

5 Application to FX markets

In this section we consider the application of the stochastic correlation model to study the correlation dynamics of the foreign exchange (FX) and the stock markets. Any cross-border trade carries a currency risk, i.e. since the exchange rate is assumed to vary randomly in time, by the time terms of the trade are fulfilled the currency rate could have changed enough to impact the parties of the trade. To hedge such risks, financial markets participants enter into specialized financial contracts like the quantity adjusting option, see Wystup 2010, wherein they can choose to lock-in the currency rate for some pre-specified terms. As we noted in Section 1 that there is work towards understanding the pricing of the quantity adjusting options where the currency and the equity are both correlated. Motivated by the interest in the problem we seek to understand the variation in the correlation dynamics of the currency market and the equity market around the world during COVID-19. It has been noted that the shock of the COVID-19 pandemic was felt unlike other previous shocks in the FX markets, Bazán-Palomino and Winkelried 2021.

We seek to study the correlation dynamics between the following pairs of exchange rates and equity indices: USD/EUR and S&P500, GBP/USD and FTSE100, INR/USD and NIFTY50, JPY/USD and NIKKEI225. Towards this we collect end of day closing data for all the pairs for the year 2020 from Yahoo Finance. We fit two models to each pair using the circular Brownian motion and the von Mises process as the correlation process. For the circular Brownian motion we set the penalization hyper-parameter $\lambda_1 = 4$ and for the von Mises process we set the hyper-parameters to $\lambda_1 = 10, \lambda_2 = 20$. We set $N = 500$ for the number of samples in the bootstrap procedure. For each pair with respect to each process, we plot the estimated correlation dynamic and the uncertainty estimate in Figures 3 and 4 respectively. On the aggregate we find the correlations estimated from both

circular Brownian motion and von Mises process to be similar except for the JPY/USD and NIKKEI225 pair. We note that the correlation dynamic estimated from the circular Brownian motion to be slightly smoother.

Across the four pairs we observe in the estimated correlation plot, that there is a shock in the correlation that aligns with the onset of COVID-19 and subsequent restrictions. In early January we see a large correlation spike and a subsequent dip for the USD/EUR and S&P500 pair which coincided with the awareness of COVID-19 in the USA. Similarly for UK and India, we see spikes in the correlation during March and April, with the onset of the COVID-19 related restrictions. We note that such a shock to the correlation doesn't persist in all the four cases.

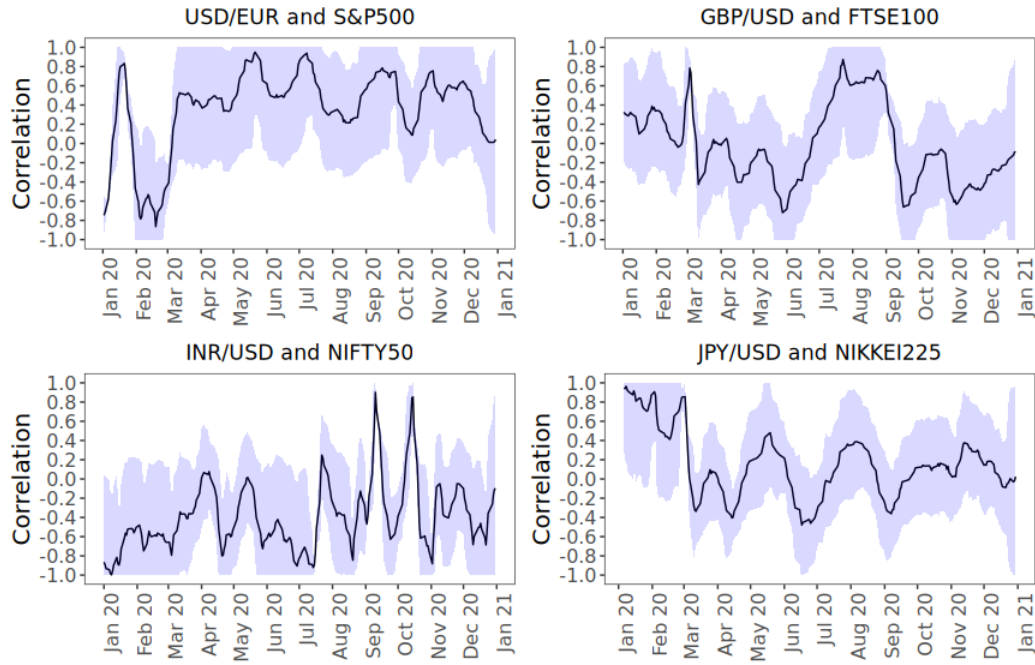


Figure 3: Plots of the estimated correlation dynamic between USD/EUR and S&P500, GBP/USD and FTSE100, INR/USD and NIFTY50, JPY/USD and NIKKEI225 for the year 2020 using circular Brownian motion as the correlation process alongwith the 95% bootstrap confidence region.

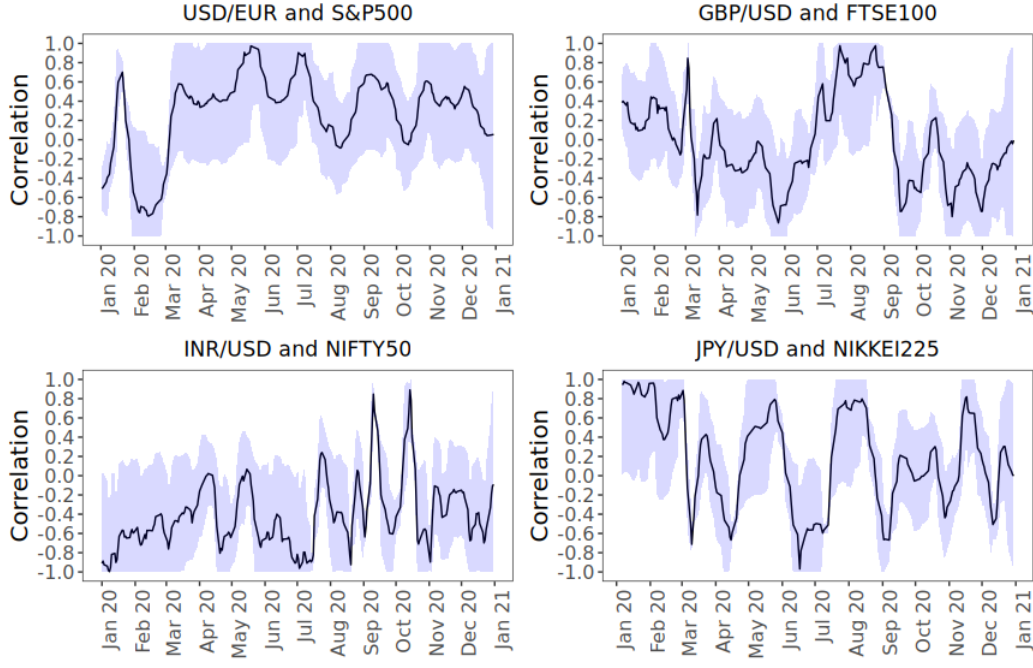


Figure 4: Plots of the estimated correlation dynamic between USD/EUR and S&P500, GBP/USD and FTSE100, INR/USD and NIFTY50, JPY/USD and NIKKEI225 for the year 2020 using the von Mises process as the correlation process alongwith the 95% bootstrap confidence region.

6 Conclusion

In this article we studied the circular Brownian motion and the von Mises process. We obtained an analytical approximation to the transition density of the von Mises process. To the best of our knowledge, this is the first reported analytical approximation to the transition density of the von Mises process, since Kent 1975 first identified the von Mises distribution as the limiting stationary distribution of the von Mises process. We proposed a novel formulation for stochastic correlation models in financial markets using diffusions on circle. We discuss the estimation of such a model. We illustrated the application of the model to the dynamics of correlation in the equity and FX markets during the COVID-19

pandemic.

We are interested in investigating multi-asset option pricing models using circular diffusions as the correlation dynamic. We hope to work on the pricing and calibration of such models to market data under the proposed correlation dynamic.

References

Aït-Sahalia, Y. (2002). Maximum likelihood estimation of discretely sampled diffusions: A closed-form approximation approach. *Econometrica*, 70(1), 223–262.

Aït-Sahalia, Y., Fan, J., & Xiu, D. (2010). High-frequency covariance estimates with noisy and asynchronous financial data. *Journal of the American Statistical Association*, 105(492), 1504–1517.

Asai, M., McAleer, M., & Yu, J. (2006). Multivariate stochastic volatility: A review. *Econometric Reviews*, 25(2-3), 145–175.

Ball, C. A., & Torous, W. N. (2000). Stochastic correlation across international stock markets. *Journal of Empirical Finance*, 7(3-4), 373–388.

Bazán-Palomino, W., & Winkelried, D. (2021). Fx markets' reactions to covid-19: Are they different? *International Economics*, 167, 50–58.

Beskos, A., Papaspiliopoulos, O., Roberts, G. O., & Fearnhead, P. (2006). Exact and computationally efficient likelihood-based estimation for discretely observed diffusion processes (with discussion). *Journal of the Royal Statistical Society Series B: Statistical Methodology*, 68(3), 333–382.

Craigmile, P., Herbei, R., Liu, G., & Schneider, G. (2023). Statistical inference for stochastic differential equations. *Wiley Interdisciplinary Reviews: Computational Statistics*, 15(2), e1585.

Driessen, J., Maenhout, P. J., & Vilkov, G. (2009). The price of correlation risk: Evidence

from equity options. *The Journal of Finance*, 64(3), 1377–1406.

Ducharme, G. R., Jhun, M., Romano, J. P., & Truong, K. N. (1985). Bootstrap confidence

cones for directional data. *Biometrika*, 72(3), 637–645.

Efron, B., & Tibshirani, R. J. (1994). *An introduction to the bootstrap*. CRC press.

Elerian, O., Chib, S., & Shephard, N. (2001). Likelihood inference for discretely observed

nonlinear diffusions. *Econometrica*, 69(4), 959–993.

Fan, J., Furger, A., & Xiu, D. (2016). Incorporating global industrial classification standard

into portfolio allocation: A simple factor-based large covariance matrix estimator

with high-frequency data. *Journal of Business & Economic Statistics*, 34(4), 489–

503.

Faria, G., Kosowski, R., & Wang, T. (2022). The correlation risk premium: International

evidence. *Journal of Banking & Finance*, 136, 106399.

Fisher, N. I., & Hall, P. (1989). Bootstrap confidence regions for directional data. *Journal*

of the American Statistical Association, 996–1002.

Fonseca, J. D., Grasselli, M., & Tebaldi, C. (2007). Option pricing when correlations are

stochastic: An analytical framework. *Review of Derivatives Research*, 10(2), 151–

180.

García-Portugués, E. (2023). *sdetorus: Statistical tools for toroidal diffusions* [R package

version 0.1.9]. <https://CRAN.R-project.org/package=sdetorus>

García-Portugués, E., Sørensen, M., Mardia, K. V., & Hamelryck, T. (2019). Langevin

diffusions on the torus: Estimation and applications. *Statistics and Computing*, 29,

1–22.

Gourieroux, C., & Sufana, R. (2010). Derivative pricing with wishart multivariate stochastic volatility. *Journal of Business & Economic Statistics*, 28(3), 438–451.

Hyvärinen, A., & Dayan, P. (2005). Estimation of non-normalized statistical models by score matching. *Journal of Machine Learning Research*, 6(4).

Itô, K. (1950). Brownian motions in a lie group. *Proceedings of the Japan Academy*, 26(8), 4–10.

Jammalamadaka, S., & Sengupta, A. (2001). *Topics in circular statistics*. World Scientific Press.

Johnson, S. G. (2007). The NLopt nonlinear-optimization package.

Kalogeropoulos, K., Dellaportas, P., & Roberts, G. O. (2011). Likelihood-based inference for correlated diffusions. *Canadian journal of statistics*, 39(1), 52–72.

Kent, J. T. (1975). Discussion of professor mardia's paper. *Journal of the Royal Statistical Society: Series B (Methodological)*, 37(3), 371–393.

Kent, J. T. (1978). Time-reversible diffusions. *Advances in Applied Probability*, 10(4), 819–835.

Khazaei, S., Ehsan, M., Soleymani, S., & Mohammadnezhad-Shourkaei, H. (2022). A high-accuracy hybrid method for short-term wind power forecasting. *Energy*, 238, 122020.

Kloeden, P. E., & Platen, E. (1992). *Numerical solution of stochastic differential equations*. Springer Berlin Heidelberg. <https://doi.org/10.1007/978-3-662-12616-5>

Kou, S., Olding, B. P., Lysy, M., & Liu, J. S. (2012). A multiresolution method for parameter estimation of diffusion processes. *Journal of the American Statistical Association*, 107(500), 1558–1574.

Lautier, D., Javaheri, A., & Galli, A. (2003). Filtering in finance. *Wilmott magazine*, 5, 67–83.

Le Cam, L. M., & Yang, G. L. (2000). *Asymptotics in statistics: Some basic concepts*.

Springer Science & Business Media.

Mardia, K. V., & Jupp, P. E. (2000). *Directional statistics*. John Wiley & Sons.

Mardia, K. V., Kent, J. T., & Laha, A. K. (2016). Score matching estimators for directional distributions. *arXiv preprint arXiv:1604.08470*.

Martin, R., Craster, R., Pannier, A., & Kearney, M. (2019). Analytical approximation to the multidimensional fokker–planck equation with steady state. *Journal of Physics A: Mathematical and Theoretical*, 52(8), 085002.

Oksendal, B. (2013). *Stochastic differential equations: An introduction with applications*. Springer Science & Business Media.

Philipov, A., & Glickman, M. E. (2006). Multivariate stochastic volatility via wishart processes. *Journal of Business & Economic Statistics*, 24(3), 313–328.

Powell, M. J. (1998). Direct search algorithms for optimization calculations. *Acta numerica*, 7, 287–336.

Prakasa Rao, B. L. S. (1983). Asymptotic theory for non-linear least squares estimator for diffusion processes. *Statistics: A Journal of Theoretical and Applied Statistics*, 14(2), 195–209.

Protter, P. E. (2005). *Stochastic integration and differential equations* (2nd ed.). Springer-Verlag.

SenGupta, A., & Roy, M. (2019). An universal, simple, circular statistics-based estimator of α for symmetric stable family. *Journal of Risk and Financial Management*, 12(4), 171.

SenGupta, A., & Roy, M. (2023). Circular-statistics-based estimators and tests for the index parameter α of distributions for high-volatility financial markets. *Journal of Risk and Financial Management*, 16(9), 405.

Sotavento Galicia. (2024). *Historical real-time data* [<https://www.sotaventogalicia.com/en/technical-area/real-time-data/historical/>, Accessed: 04-12-2024].

Stillwell, J. (2008). *Naive lie theory*. Springer New York.

Teng, L., Ehrhardt, M., & Günther, M. (2015). The pricing of quanto options under dynamic correlation. *Journal of Computational and Applied Mathematics*, 275, 304–310.

Teng, L., Ehrhardt, M., & Günther, M. (2016a). Modelling stochastic correlation. *Journal of Mathematics in Industry*, 6, 1–18.

Teng, L., Ehrhardt, M., & Günther, M. (2016b). On the heston model with stochastic correlation. *International Journal of Theoretical and Applied Finance*, 19(06), 1650033.

Teng, L., Ehrhardt, M., & Günther, M. (2018). Quanto pricing in stochastic correlation models. *International Journal of Theoretical and Applied Finance*, 21(05), 1850038.

Van Emmerich, C. (2006). Modelling correlation as a stochastic process. *Preprint*, (06/03).

Wystup, U. (2010). Quanto options. In *Encyclopedia of quantitative finance*. John Wiley & Sons, Ltd. <https://onlinelibrary.wiley.com/doi/10.1002/9780470061602.eqf06006>

Yoshida, N. (1992). Estimation for diffusion processes from discrete observation. *Journal of Multivariate Analysis*, 41(2), 220–242.

A Proof of Lemma 2.1

Let X be a d -dimensional Riemannian manifold with metric tensor $g(x)$. Let $f(x)$ be a smooth, strictly positive density on X . The characteristic diffusion of f , i.e., the diffusion

for which $f(x)$ is its stationary density is given by the pair (G, B) (Kent 1978, Theorem 10.1):

$$G = \Delta + \sum_i b_i(x) \frac{\partial}{\partial x_i} \quad (24)$$

where B is the periodic boundary condition. Here G is the infinitesimal generator of the diffusion. More general forms of B are also admissible, see p. 821 Kent 1978. Here $b_i(x) = \sum_{j=1}^d g_{ij}^{-1} \frac{\partial \log f}{\partial x_j}$ and Δ is the Laplace-Beltrami operator on X . The Laplace-Beltrami operator on X is given by,

$$\Delta = \delta^{1/2}(x) \sum_{i,j} \frac{\partial}{\partial x_i} \left[\delta^{-1/2}(x) g_{ij}(x) \frac{\partial}{\partial x_j} \right]$$

where $\delta(x) = \det g^{-1}(x)$.

The Laplace-Beltrami operator on the unit circle is given by,

$$\Delta = \frac{\partial^2}{\partial \theta^2}$$

Therefore the Kolmogorov backward equation is,

$$\frac{\partial p^*}{\partial t} = G p^*$$

and hence,

$$\frac{\partial p^*}{\partial t} = \frac{\sigma^2}{2} \frac{\partial p^*}{\partial \theta^2} + \frac{\partial \log f}{\partial \theta} \frac{\partial p^*}{\partial \theta}$$

and collecting the coefficients for the drift and the diffusion term on the RHS, we obtain the SDE.

B Proof of Theorem 2.2

For a SDE,

$$dY_t = \nu A(Y_t)dt + \sqrt{2\nu}dB_t \quad (25)$$

the corresponding forward equation is given by,

$$\frac{\partial f}{\partial \tau} = -\frac{\partial}{\partial y}[A(y)f] + \frac{\partial^2 f}{\partial y^2} \quad (26)$$

where τ is the nondimensional time, with $\tau = \nu t$. The stationary density $f_e(y) \propto \exp \int A(z)dz$.

Then for $f(\tau, y) = g(\tau, y)f_e(y)$, the adjoint equation is,

$$\frac{\partial g}{\partial \tau} = A(y)\frac{\partial g}{\partial y} + \frac{\partial^2 g}{\partial y^2} \quad (27)$$

It follows that for $h = -\left(\frac{\partial}{\partial y}\right) \log g$, h satisfies the PDE,

$$\frac{\partial h}{\partial \tau} = \frac{\partial}{\partial y} \left\{ A(y)h + \frac{\partial h}{\partial y} - h^2 \right\} \quad (28)$$

Consider an Ornstein-Uhlenbeck process,

$$dy_t = \nu\gamma(a - y_t)dt + \sqrt{2\nu}dB_t$$

For the OU process $A(y) = \gamma(a - y)$ and h is known in closed form for the OU process,

$$h(\tau, y) = \frac{\gamma\sqrt{q}(y - y_0)}{1 - q} + \frac{\gamma\sqrt{q}(a - y)}{1 + \sqrt{q}}$$

where $q = \exp(-2\gamma\tau)$. Notice that it can alternatively be expressed as,

$$h(\tau, y) = \frac{\gamma\sqrt{q}(y - y_0)}{1 - q} + \frac{\sqrt{q}A(y)}{1 + \sqrt{q}} \quad (29)$$

for $A(y) = \gamma(a - y)$. This form is used then as an ansatz for the solution to the forward equation for the von Mises process,

$$h^*(\tau, y) = \frac{\gamma\sqrt{q}(y - y_0)}{1 - q} + \frac{\sqrt{q}A(y)}{1 + \sqrt{q}} + \sqrt{q}o(1)_{q=1} \quad (30)$$

It is argued in Martin et al. 2019, p. 5 that as $\tau \rightarrow 0$, i.e. $q \rightarrow 1$, the error term is of the order $o(1)$, which is what $o(1)_{q=1}$ denotes. γ is an artefact from the specification of the OU process. We need to identify a suitable value for γ for the von Mises process. Towards this an expansion of the remainder term is considered,

$$h^*(\tau, y) = \frac{\gamma\sqrt{q}(y - y_0)}{1 - q} + \frac{\sqrt{q}A(y)}{1 + \sqrt{q}} + \frac{\sqrt{q}}{1 + \sqrt{q}} \sum_{i=1}^{\infty} (1 - \sqrt{q})^i b_i(y)$$

We note that,

$$b_1(y) = \frac{1}{\gamma(y - y_0)^2} \int_{y_0}^y (s - y_0) \left[\frac{d^2}{ds^2} (A(s) + \gamma s) + \left(A(s) + \frac{\gamma(s - y_0)}{2} \right) \left(\frac{d}{ds} (A(s) + \gamma s) \right) \right] ds \quad (31)$$

Observe that $b_1(y) = 0$ if $A'(y) + \gamma = 0$. This motivates the following choice for γ ,

$$\gamma = \mathbb{E}_{f_e}[-A'(y)] \quad (32)$$

where f_e is the stationary distribution of the process. For the von Mises process,

$$A(\theta) = -\frac{2\lambda}{\sigma^2} \sin(\theta - \mu) \quad (33)$$

and $f_e = \frac{1}{2\pi I_0(\kappa)} \exp(\kappa \cos(\theta - \mu))$. Therefore,

$$\gamma = \int_{-\pi}^{\pi} \kappa \cos(\theta - \mu) \frac{\exp(\kappa \cos(\theta - \mu))}{2\pi I_0(\kappa)} d\theta = \kappa \frac{I_1(\kappa)}{I_0(\kappa)} \quad (34)$$

Plugging expressions (33) and (34) for von Mises process into (30) and we obtain,

$$f(\theta_\tau; \theta_0) \propto \exp\left(\frac{-\gamma\sqrt{q}(\theta_\tau - \theta_0)^2}{2(1-q)}\right) \left(\frac{1}{2\pi I_0(\kappa)}\right)^{\frac{1-\sqrt{q}}{1+\sqrt{q}}} \exp\left(\frac{\kappa(\cos(\theta_\tau - \mu) - \sqrt{q}\cos(\theta_0 - \mu))}{1+\sqrt{q}}\right) \quad (35)$$

To accommodate the periodic boundary conditions, we wrap (35) to obtain the approximate transition probability density of the von Mises process,

$$p(\theta_t; \theta_0) \propto \sum_{k=-\infty}^{\infty} \exp\left(\frac{-\gamma\sqrt{q}(\theta_t + 2\pi k - \theta_0)^2}{2(1-q)}\right) \left(\frac{1}{2\pi I_0(\kappa)}\right)^{\frac{1-\sqrt{q}}{1+\sqrt{q}}} \exp\left(\frac{\kappa(\cos(\theta_t - \mu) - \sqrt{q}\cos(\theta_0 - \mu))}{1+\sqrt{q}}\right) \quad (36)$$

where $\gamma = \kappa(I_1(\kappa)/I_0(\kappa))$ and $q = \exp(-\gamma\sigma^2 t)$. We note that as $t \rightarrow \infty$, $p(\theta_t; \theta_0) \rightarrow f_e$, which is the expected theoretical stationary distribution.

C Proof of Theorem 4.1

C.1 Preliminaries

In this section we consider the existence of strong solution of the following system of SDEs,

$$dS_t^{(1)} = \mu^{(1)}S_t^{(1)}dt + \sigma^{(1)}S_t^{(1)}dW_t^{(1)} \quad (37)$$

$$dS_t^{(2)} = \mu^{(2)}S_t^{(2)}dt + \sigma^{(2)}S_t^{(2)}(\rho_t dW_t^{(1)} + \sqrt{1-\rho_t^2}dW_t^{(2)}) \quad (38)$$

$$d\theta_t = -\lambda \sin(\theta_t - \mu)dt + \sigma dW_t^{(3)} \quad (39)$$

Here $W_t^{(1)}, W_t^{(2)}, W_t^{(3)}$ are mutually independent Brownian motions and $\rho_t = \cos \theta_t$. The existence of strong solution of (37) and (39) follows from the standard theory of Lipschitz coefficients. We will prove that (38) admits a strong solution. We will require the following version of the Grönwall's inequality,

Lemma C.1. *Let $y_n(t)$ be a sequence of nonnegative functions such that for some constants $B, C < \infty$, $y_0(t) \leq C, \forall t \leq T$ and $y_{n+1}(t) \leq B \int_0^t y_n(s)ds < \infty, \forall t \leq T, n \in \mathbb{N}$. Then,*

$$y_n(t) \leq \frac{CB^n t^n}{n!}, \forall t \leq T$$

C.2 Strong solution

We will rewrite (38) in the following manner to ease on the notation,

$$dS(t) = \mu S(t)dt + \sigma S(t)(\rho(t)dW^{(1)}(t) + \sqrt{1 - \rho^2(t)}dW^{(2)}(t)) \quad (40)$$

Consider the initial condition $S(0) = S$ and a compact time interval $[0, T]$. We next consider the Picard's iterations of (40). Therefore for some $t \in [0, T]$,

$$S_0(t) \equiv S$$

$$S_{n+1}(t) = S + \int_0^t \mu S_n(u)du + \int_0^t \sigma S_n(u)(\rho(u)dW^{(1)}(u) + \sqrt{1 - \rho^2(u)}dW^{(2)}(u)), \forall n \in \mathbb{N}$$

We will next show that $S_n(t)$ converges in L^2 .

$$\begin{aligned}
& \mathbb{E}[(S_n(t) - S_{n-1}(t))^2] \\
&= \mathbb{E} \left[\left(\int_0^t \mu(S_n(u) - S_{n-1}(u))du + \int_0^t \sigma(S_n(u) - S_{n-1}(u))(\rho(u)dW^{(1)}(u) + \sqrt{1 - \rho^2(u)}dW^{(2)}(u)) \right)^2 \right] \\
&\leq 4\mathbb{E} \left[\left(\int_0^t \mu(S_n(u) - S_{n-1}(u))du \right)^2 \right] + 4\mathbb{E} \left[\left(\int_0^t \sigma\rho(u)(S_n(u) - S_{n-1}(u))dW^{(1)}(u) \right)^2 \right] \\
&\quad + 4\mathbb{E} \left[\left(\int_0^t \sigma\sqrt{1 - \rho^2(u)}(S_n(u) - S_{n-1}(u))dW^{(1)}(u) \right)^2 \right]
\end{aligned}$$

(Follows from $(x + y + z)^2 \leq 4x^2 + 4y^2 + 4z^2$)

$$\begin{aligned}
&\leq 4\mathbb{E} \left[t \int_0^t \mu^2(S_n(u) - S_{n-1}(u))^2 du \right] + 4\mathbb{E} \left[\int_0^t \sigma^2\rho^2(u)(S_n(u) - S_{n-1}(u))^2 du \right] \\
&\quad + 4\mathbb{E} \left[\int_0^t \sigma^2(1 - \rho^2(u))(S_n(u) - S_{n-1}(u))^2 du \right]
\end{aligned}$$

(Applying Cauchy-Schwarz inequality to the first term and

Itô's isometry to the second and third term)

$$\leq 4K(t+1)\mathbb{E} \left[\int_0^t (S_n(u) - S_{n-1}(u))^2 du \right]$$

$(\exists K > \max(\mu^2, \sigma^2))$

$$= 4K(t+1) \int_0^t \mathbb{E}[(S_n(u) - S_{n-1}(u))^2] du$$

From Lemma C.1,

$$\mathbb{E}[(S_{n+1}(u) - S_n(u))^2] \leq \frac{C(4K(t+1))^n}{n!} \quad (41)$$

Therefore, $\exists S(t)$ such that,

$$\lim_{n \rightarrow \infty} \mathbb{E}[(S_n(t) - S(t))^2] = 0 \quad (42)$$

for $t \in [0, T]$.

It also follows that,

$$\lim_{n \rightarrow \infty} \mathbb{E} [(\mu(S_n(t) - S(t)))^2] = 0 \quad (43)$$

$$\lim_{n \rightarrow \infty} \mathbb{E} [(\sigma \rho(u)(S_n(t) - S(t)))^2] \leq \lim_{n \rightarrow \infty} \mathbb{E} [(\sigma(S_n(t) - S(t)))^2] = 0 \quad (44)$$

$$\lim_{n \rightarrow \infty} \mathbb{E} [(\sigma \sqrt{1 - \rho^2(u)}(S_n(t) - S(t)))^2] \leq \lim_{n \rightarrow \infty} \mathbb{E} [(\sigma(S_n(t) - S(t)))^2] = 0 \quad (45)$$

((44) and (45) follows since $|\rho(u)| \leq 1$)

We will next show that $S(t)$ satisfies (40). Consider,

$$\begin{aligned} & \lim_{n \rightarrow \infty} \mathbb{E} \left[\left(\int_0^t \mu(S_n(u) - S(u)) du \right)^2 \right] \\ & \leq \lim_{n \rightarrow \infty} \mathbb{E} \left[t \int_0^t (\mu(S_n(u) - S(u)))^2 du \right] \\ & \quad (\text{Using Cauchy-Schwarz inequality}) \\ & = \lim_{n \rightarrow \infty} \int_0^t t \mathbb{E} [(\mu(S_n(u) - S(u)))^2] du = 0 \quad (46) \\ & \quad (\text{From (43)}) \end{aligned}$$

From (46) it follows that the drift term of (40) converges in L^2 . Next consider,

$$\begin{aligned} & \lim_{n \rightarrow \infty} \mathbb{E} \left[\left(\int_0^t \sigma \rho(u)(S_n(u) - S(u)) dW^{(1)}(u) \right)^2 \right] \\ & = \lim_{n \rightarrow \infty} \mathbb{E} \left[\int_0^t (\sigma \rho(u)(S_n(u) - S(u)))^2 du \right] \\ & \quad (\text{Using Itô's isometry}) \\ & \leq \lim_{n \rightarrow \infty} \int_0^t \mathbb{E} [(\sigma(S_n(u) - S(u)))^2] du = 0 \quad (47) \\ & \quad (\text{From (44) and } |\rho(u)| \leq 1) \end{aligned}$$

Similarly, we can show that,

$$\lim_{n \rightarrow \infty} \mathbb{E} \left[\left(\int_0^t \sigma \sqrt{1 - \rho^2(u)}(S_n(u) - S(u)) dW^{(2)}(u) \right)^2 \right] = 0 \quad (48)$$

From (47) and (48) it follows that the diffusion terms of (40) converge in L^2 .